Hydro-Catalytic Cracking of Biomass Tar Contamination in Syngas

by Amal Fiaz

Submission date: 25-Aug-2024 08:58PM (UTC-0500)
Submission ID: 2438024744
File name: Naskah_Aris_11.pdf (988.57K)
Word count: 7957
Character count: 40066

RiESTech
Recent in Engineering Science and Technology

MBI

Article

Hydro-Catalytic Cracking of Biomass Tar Contamination in Syngas

Aris Warsita [1], Hasta Kuntara [2], Zainal Abidin [3]

[1] Department of Mechanical Engineering, Insititut Teknologi Nasional Yogyakarta, Jl. Babarsari Caturtunggal, Depok, Sleman, 55281 Yogyakarta, Indonesia
[2] Department of Mechanical Engineering, Universiti Sains Malaysia Penang, Malaysia
* Correspondence: ariswarsita@itny.ac.id

Abstract: This paper describes new tar removal augmentation method by adding water that enhances the steam reformation reactions and converts tar contamination in the gas into combustible gases. The hydro-catalytic tar removal method was experimentally evaluated in a microwave-heated reactor with toluene and naphthalene as tar models. The reactor was tested in a wide temperature range with flow residence time through the reactor in the range of 0.12-0.24s. Dolomite and nickel catalysts were tested at 700-900°C while Y-zeolite, ruthenium, and rhodium were tested at 500-700°C temperature ranges. Steam-to-carbon ratio (S/C) was tested in the range of 0.11-0.55. Tar removal efficiency of 98.88% was achieved with ruthenium catalyst at 700 °C cracking temperature and S/C ratio range of 0.32-0.33. The gas product from tar cracking was analysed using gas chromatography and it consisted mostly of H2, CH4 and some higher hydrocarbon gases.

Keywords: Hydro-catalytic tar removal; Microwave irradiation; Thermal tar cracking; Naphthalene conversion; Toluene conversion

Citation:. Warsita, A., Kuntara, H., Abidin., Z. (2024). Hydro-Catalytic Cracking of Biomass Tar Contamination in Syngas. Recent in Engineering Science and Technology, 2(02), 18–34. Retrieved from https://www.mbi-journals.com/index.php/riestech/article/view/51

Academic Editor: Iwan Susanto

Received: 18 March 2024
Accepted: 6 April 2024
Published: 30 April 2024

1. Introduction

The conversion of solid biomass fuel into more convenient synthesis gas (syngas) with its neutral effect on global warming has been elaborately investigated for many decades [1,2]. Biomass syngas, unlike another type of renewable energy resources, can be utilized directly in most of the existing power plants without major modification by co-firing with fossil fuels. This option has been considered in many countries due to its positive effect on large scale electrical generation carbon footprint reduction. However, one of the major obstacles in syngas utilization is its high tar contamination that can cause blockage and fouling in fuel-feeding equipment. Moreover, tar has negative effect on fuel cells, reciprocating internal combustion (IC) engine and gas turbines in the long-term operation causing corrosion and fouling that can reduce engines life and increase maintenance cost [3,4]. Although steam boilers have higher tolerance to tar contamination, IC engines and gas turbines are sensitive to tar contamination and can accept only below 100 and 5 mg Nm^{-3} respectively [5]. Therefore, in subsequent utilization of syngas fuel, tar must be eliminated by converting it into useful gases.

Tar removal technology can be divided into two groups: removal inside the gasifier known as the primary method and the removal after the gasifier known as the secondary method [6]. Primary method is one of the oldest techniques of tar cracking and it has the advantage of eliminating any tar removal equipment after the gasifier, but with limited tar elimination capability [7,8]. On the other hand, heating, catalytic reaction and mechanical separation using a cyclone, filter and scrubber are common means of the secondary tar removal method.

Catalytic tar cracking with steam reforming during the gasification process is widely investigated [9,10]. Wide range of catalytic materials were tested in the primary method such as Ni, Al, Ru, Rh, Pt, Pd, Al_2O_3, ZrO_2, TiO_2, SiO_2, MOR1, CeO_2, ZrO_2 and MgO [11,12]. Dolomite is widely used as a non-metallic catalyst for the conversion of tar [13-15]. Dolomite calcination treatment is essential to achieve good tar conversion activity [16], and the effect also depends on the source of the natural dolomite [17,18]. However it has a low friction resistance and is easy to be carried away making it unfit for use in fluidized bed reactors. Olivine is another natural mineral which has shown higher activity in tar conversion [13,19]. When compared with dolomite, olivine has a high friction resistance which allows its direct use as the primary catalyst in fluidized bed gasifiers. The use of Y-zeolite for the conversion of biomass tar has also been reported but to a lesser extent [20-22].

As for the secondary tar removal in a separate reactor after the gasifier, the use of catalysts require temperature range of 500-900 ^{0}C making it more attainable both technically and economically. Also, tar is converted into combustible gases such as H_2, CH_4 and CO that enhances the quality of syngas. Various catalyst types such as Fe, Cu, Co and Ni based catalysts, dolomite, olivine and Y-zeolite were widely investigated [23-25].

Microwave irradiation is an alternative heating method which has been successfully applied to biomass pyrolysis [26,27]. Compared with conventional heating where heat is transferred from the surface to the core of the material by conduction driven by the temperature gradient, microwaves induce heat at the molecular level by direct conversion of electromagnetic energy into heat [28]. and results in uniform heating for particulate material. Another advantage is instantaneous response for fast microwave start-up and shutdown.

Microwave assisted thermal and catalytic syngas tar cracking has been widely investigated as well. Dolomite, Y-zeolite [29,30], bio-char [31] and bio-char with K and Ca [32] catalysts, as well as silicon carbide (SiC) [29, 30, 33] as micro wave radio frequency absorbing material have been studied. Most of the studies used tar model materials to simulate the different grades of biomass tar for better control over the quantities of tar with only few studies on actual tar from biomass gasification [30]. Common materials used as tar models are toluene, naphthalene, phenol, benzene, and 1-Methylnaphthalene [29-36].

In the current study, a new concept of hydro-catalytic tar removal in a post-gasification syngas treatment was experimentally investigated. The combined effect of water and catalytic materials in microwave assisted thermal cracking is fully characterized. Wide range of catalysts: dolomite, Y-zeolite, nickel, ruthenium, and rhodium were tested separately with different water-tar ratios to obtain maximum tar removal.

2. Materials and Experiment Methods

2.1. Materials and Catalytic Calcination

In this study, actual syngas from biomass gasification was not used to evaluate the methods of tar removal due to the continuous fluctuation in tar concentration. Therefore, toluene and naphthalene (commercial grade) tar models were used for better control and accurate measurement of tar removal. Naphthalene ($C_{10}H_8$) is a lightweight poly-aromatic hydrocarbons (LPAH) consists of two fused benzene rings and it is a class 4 tar while toluene (C_7H_8) is a light aromatic hydrocarbon (LAH) with a ring compound which is a class 3 tar. Both classes 3 and 4 tar are classified as the main tar products from biomass

gasification in fluidized bed and downdraft gasifiers. Purified nitrogen (99.999%) was used as a carrier gas to transfer tar model vapours through the tar cracking reactor.

Tar formed in the pyrolysis zone inside the gasifier is one of the main sources of tar, thus, catalytic pyrolysis has attracted much attention as a promising potential in tar reduction [35]. However, catalytic materials have to go through calcination process at elevated temperature to achieve the desired effect. In this study, five catalytic materials: dolomite, Y-zeolite, nickel, ruthenium and rhodium were investigated for tar removal. Commonly, the use of support materials for nickel catalyst such as alumina, zeolite, dolomite and olivine has been widely studied in literatures due to their positive effect on tar removal as well as increasing the pore size and surface area. However, pure nickel was used in this study to provide more controlled environment to test its effect on tar cracking without any support materials. Dolomite has a particle size of 600 μm with a bulk density of 1.33 g cm^{-3}. It is mainly composed of 34.69 wt.% CaO, 15.06 wt.% MgO and 2.34 wt.% SiO_2. Y-zeolite is a commercial catalyst powder (CBV720) with a bulk density of 0.26 g cm-3 and SiO_2/Al_2O_3 of 30. Commercial nickel 257 553, Aldrich is a mix of metal, with a thickness of 0.5 mm, bp 2733 ^{0}C, mp 1453 ^{0}C and density of 8.9 g/ml at 25 ^{0}C. Commercial ruthenium 246047-72-3 with $C_{46}H_{65}C_{l2}N_2PRu$, and 848.97 g.mol^{-1}. Commercial rhodium $C_{17}H_{18}NORh$ 33409-86-3, and has a molecular weight of 355.24 g.mol^{-1}. The process of making natural dolomite included grounding and sieving with output particle sizes in the range of 0.2-0.5 mm, followed by calcination. Calcination of dolomite is needed for high tar decomposition activity since it has large surface area and oxide content on the surface. H_2 content in the producer gas can be more improved with the use of calcined dolomite as downstream catalytic steam gasification compared to that of uncalcined dolomite [37]. The effect of calcination was widely in literatures as reviewed by Anis and Zainal [6] and has shown a positive improvement in catalyst activity. A muffle oven with air flow was used for dolomite and nickel calcination at 900 ^{0}C for 1 hour and at 600 ^{0}C for 2 hours for Y-zeolite,

ruthenium and rhodium. Table 1 shows the catalytic materials specifications and calcination processes.

Table 1. Characteristics of catalysts

Properties	Value	Properties	Value
Y-zeolite		**Ruthenium**	
SiO_2/Al_2O_3	30	assay	99.98% trace metals basis
Na_2O	0.03% (wt.%)	form	powder and chunks
Unit cell size (Å)	24.28	Calcination	600 °C for 2h under air flow
Surface Area	780 (m^2/g)	**Rhodium**	
Pore size (Å)	7.4	assay	99.95% trace metals basis
density	0.26 ($g\ m^{-3}$)	form	powder
Calcination	600 °C for 2 h under air flow	resistivity	4.33 $\mu\Omega^{-cm}$ at 20 °C
Dolomite		density	12.41 g/cm^3
Composition (wt.%)	34.69% CaO, 15.06% MgO, 2.34% SiO_2, 1.07% Al_2O_3, 0.61% Fe_2O_3	Calcination	600 °C for 2 h under air flow
Particle size	600 (µm)		
density	1.33 ($g\ m^{-3}$)		
Calcination	900 °C for 1h under air flow		
Nickel			
assay	99.7% trace metals basis		
form	powder		
resistivity	6.97 $\mu\Omega^{-cm}$, 20 °C		
particle size	<50 µm		
density	8.9 g/mL at 25 °C		
Calcination	900 °C for 1h under air flow		

Carbon based susceptor materials has the ability to absorb radio frequency and convert it into heat. Charcoal is one of the commonly used susceptor materials. However, it was not used in this study due to its additional effect as a catalyst that will interfere with the measurement of the catalytic effect of other materials. Silicon carbide (SiC) was used instead as the susceptor material. Four SiC particle sizes were compared: 2.085mm (F10), 1.765 mm (F12), 1.470 mm (F14) and 1.230 mm (F16) to investigate the effect of particle sizes on radio frequency penetration depth and heat generation.

2.2. Experimental Procedures and Equipment

The experimental test rig was developed in a previous study to investigate the hydrothermal cracking of tar without catalysts. The experimental test rig consists of the tar vapour/steam generator, mixing chamber, ceramic tube reactor, microwave oven and tar/gas sampling train. Four type-K thermocouples are used for temperature measurement at different parts of the system as shown in Figure 1. A predetermined tar/water mass is placed in a stainless steel (SS) insulated container for tar evaporation and steam generation. LPG stove is used to provide the required heat for boiling, and the temperature is maintained at 250°C throughout the test to achieve homogenous mixing between tar and steam. Pressurized nitrogen is used as a carrier gas to control the flow residence time through the reactor. In order to insure the mixture homogeneity, tar vapour/steam flow is mixed with nitrogen in a SS insulated mixing chamber, and the temperature is maintained at 200°C

using hot-plate induction heater. Details of the system design and the tar/gas sampling train were published [38].

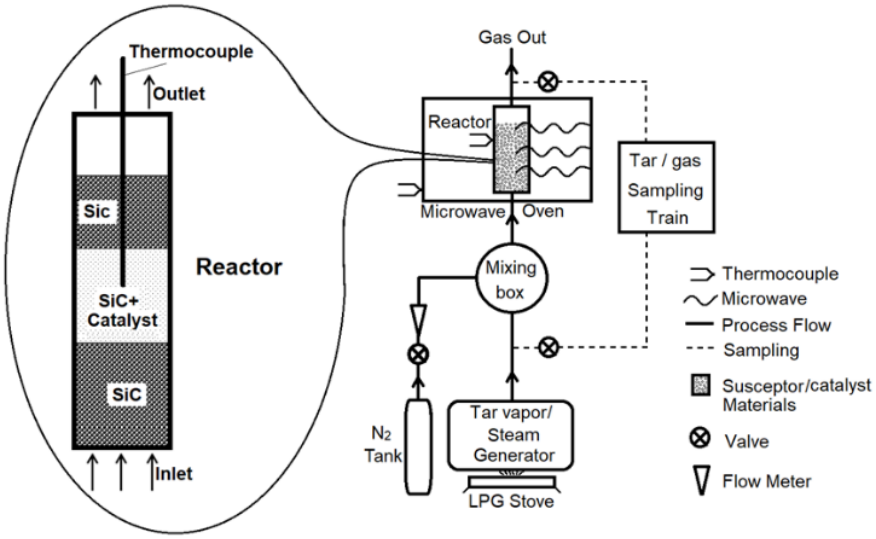

Figure 1. Schematic diagram of the experiment test rig

In this investigation, three sets of experiments were performed. First, the rector was characterised with SiC as the reactor bed material by passing N_2 carrier gas only without the addition of water, tar and catalytic materials. Four main variables were compared: SiC particle size, bed height, N_2 flow rate, and microwave electrical input power. Power absorption efficiency of the microwave oven was calculated as the ratio of the actual absorbed power by the bed material to the electrical power input. The absorbed power (Pabs) is calculated according to Equation (1) [39]:

$$\boldsymbol{P_{abs} = \rho c_p \frac{(T-T_{inlet})}{t} V + h_i A(T - T_{inlet}) + \varepsilon \sigma A \bar{T}^4} \quad \textbf{(1)}$$

where T, Tinlet and T¯are the reaction temperature (K), reactor inlet temperature (K) and the average temperature within the reactor (K), respectively whilst t is the irradiation time period (s), r is the density of absorber material (kg m-3), cp is the heat capacity of absorber material (J kg-1 K-1), hi is the convective heat transfer coefficient (W m-2 K-1), is the emissivity of absorber material and is Stefan-Boltzman constant (5.67 x 10-8 W m-2 K-4) and A is the reactor wall surface area.

The second set of experiments investigated the effect of water addition on tar cracking with different types of catalytic materials. In order to provide a controlled environment, all the catalysts were used in their pure form as an active catalyst without the addition of any promoter or support materials to increase the pore size or surface area and enhance tar cracking. Therefore, nickel and other metals were used in their pure form without any support materials. This will reduce naturally their performance due to their non-pours nature and lower surface area.

Tar cracking efficiency was calculated as the ratio of mass of the tar model obtained from the tar sampling train before and after passing the reactor. Main investigated variables for each catalyst were the steam-to-carbon (S/C) mass ratio and cracking temperature in the

range of 500-900 ^{0}C. S/C ratio was chosen over the water-to-tar ratio used in other studies [38] due to the variation in carbon mass % in tar as it presents 93.8% in naphthalene compared to 91.3% in toluene. The tested S/C ratio values for toluene were 0.11, 0.22, 0.33, 0.44, 0.55 and for naphthalene were 0.1, 0.21, 0.32, 0.43, 0.53.

The third set of experiments included the analysis of the gas product from the reactor at different cracking temperatures. Different types of catalytic materials were tested with the optimum S/C ratio obtained from the second set of experiments. The gas product is basically generated by the thermal catalytic cracking of the tar model additional to the steam reactions. Gas compositions and heating value were determined using gas chromatography (GC). The experiments provided the optimum operation conditions to achieve maximum heating value of the gas product.

2.3. Tar Hydro-Catalytic Cracking

The use of thermal cracking as the only mean for tar cracking is not efficient due to the lack of oxygen content in the light aromatic and light poly-aromatic hydrocarbons that are classified into classes 3 and 4 tar mainly from downdraft gasifiers. Thus, using catalysts containing free oxygen has shown positive effect on tar cracking and preventing coke formation [40]. Other than the free oxygen, CO_2 can also be used as an agent but in highly endothermic reactions. Equations (2 6) show the common reactions associated with the reduction of tar using O_2 and CO_2 agents [41,42].

Oxidation: $C + O_2 \leftrightarrow CO_2 + 393$ kJ.mol-1 (2)

Partial oxidation: $C + 1/2O_2 \leftrightarrow CO + 110$ kJ.mol-1 (3)

Boudouard reaction: $C + CO_2 \leftrightarrow 2CO -$ 173.8 kJ.mol-1 (4)

Dry reforming: $CH4+CO_2 \leftrightarrow 2CO+2H_2 -$ 247.3 kJ.mol-1 (5)

Methanation: $C + 2H_2 \leftrightarrow CH_4 +74.82$ kJ.mol-1 (6)

Steam gasification can produce syngas with a considerably higher heating value compared to air gasification which is mainly cause by the increment in H_2 concentration in the product gas. Similarly, the addition of water at elevated temperature inside the reactor initiates steam reaction with tar that produces H_2 [43] as illustrated in Equations

(7 11) [36]. Tar model also cracks into methane that reacts with water in steam reforming reactions as shown in Equations (12, 13) forming H2 as part of the gas product from the reactor. Toluene and naphthalene steam reforming reactions:

$$C_7H_8 + 7H_2O \rightarrow 7CO + 11H_2 \quad (7)$$

$$C_{10}H_8 + 10H_2O \leftrightarrow 10CO + 14H_2 \quad (8)$$

Heterogeneous water gas reaction: $C + H_2O \leftrightarrow CO + H \quad -118.9\ kJ.mol^{-1}$ (9)

$$C + 2H_2O \leftrightarrow CO_2 + 2H_2 - 90.2\ kJ.mol^{-1} \quad (10)$$

Homogeneous water gas shift reaction: $CO + H_2O \leftrightarrow CO_2 + H_2 + 40\ kJ.mol^{-1}$ (11)

Methane steam reforming reactions:

Primary: $CH_4 + H_2O \leftrightarrow CO + 3H_2 - 206.3\ kJ.mol^{-1}$ (12)

Secondary: $CH_4 + 2H_2O \leftrightarrow CO_2 + 4H_2 - 165\ kJ.mol^{-1}$ (13)

It can be noticed that CO formation is mainly through endothermic reactions either by the steam or dry reforming reactions or the Boudouard reaction. Thus, reaction sustainability and equilibrium is highly dependent on the heat supply to the reaction and reaction temperature.

2.4. Tar and Product Gas Analysis

Tar samples before and after the passing the reactor were condensed at 22 ^{0}C in the sampling train while gas product after the reactor was collected in gas sampling bags. Gas product was analysed using GC model CP 4900 with a thermal conductivity detector (TCD). Tar samples were analysed using gas chromatography/mass spectrometry (GC-MS) model 7890-5975C Agilent with HP-5 MS capillary column. Helium was used as carrier gas at a flow rate of 1.2 mL/min. The size was 1 µL injection with a split ratio of 1:10.40 ^{0}C initial oven temperature was held for 3 minutes and then increased to 290 ^{0}C at a rate of 5 ^{0}C/min, and held at 290 ^{0}C for 5 minutes while the injector and detector were maintained at a constant temperature of 230-250 ^{0}C.

For gas product, H^2, CO, CO^2, CH_4 and N_2 gas concentrations were detected by GC while the C_2-C_3 hydrocarbons were not detected. Nitrogen flow rate was always fixed during the tests, thus, the change in the average N2 concentration was determined by calculating the results of H_2, CO, CO^2 and CH_4 concentration in each time trial. Based on the product

gas, the conversion of toluene (xC_7H_8) was calculated according to Equation (14) in terms of carbon in the product gas (CO, CO_2, CH_4)p divided by the carbon in toluene.

$$\mathbf{X_c} = \frac{[CO]p + [CO_2]p + [CH_4]p}{7[C_7H_8]inlet} \quad (14)$$

An example of the calculation of hydrogen product by the potential stoichiometry corresponding to the total conversion of toluene into H_2 is shown in Equation (15), where hydrogen concentration [H_2] is taken from GC results. Other gases are calculated similarly.

$$[H_2]p = [H_2] \times 18[C_7H_8]inlet \quad (15)$$

Sulfur-compounds contamination in gas product such as H_2S are prominent in coal gasification with sulfur deposits issues on the catalyst surfaces that can lead to catalyst deactivation. However, this issue is nearly prevented by biomass gasification with low sulfur contamination, thus, sulfur-compounds were not considered in this study.

3. Results and Discussion

Preliminary set of experiments included the thermal characterization of the reactor and the optimum operation conditions of the reactor were utilized for tar removal optimization. The most effective catalyst and the optimum S/C ratio were used subsequently to characterize the tar reduction and product gas quality.

3.1. Thermal Characteristic of Microwave Reactor

The aim of these set of experiments was to obtain the optimum thermal cracking conditions for the reactor without including tar models and catalytic materials. The main tested reactor variables were: SiC particles sizes, SiC bed height, N2 gas flow rate, microwave input power.

3.1.1.Effect of absorber material particle size

Four SiC particle sizes were tested while fixing other variables at 700 W input power, 10 LPM N_2 flow rate, and maximum bed height of 120 mm. Figure 2a shows the power absorption efficiencies for each absorber bed material particle sizes. Results showed that the average absorption efficiencies were 87%, 88%, 91% and 93% for F10, F12, F14 and F16 sizes, respectively. In general, the difference was less than 5% on average, indicating that for all particle sizes, the microwave energy was enough to penetrate into the particles and might only focus on one hotspot. Since SiC absorber particle size of F16 provided good efficiency and temperature, this size was used in subsequent experiments.

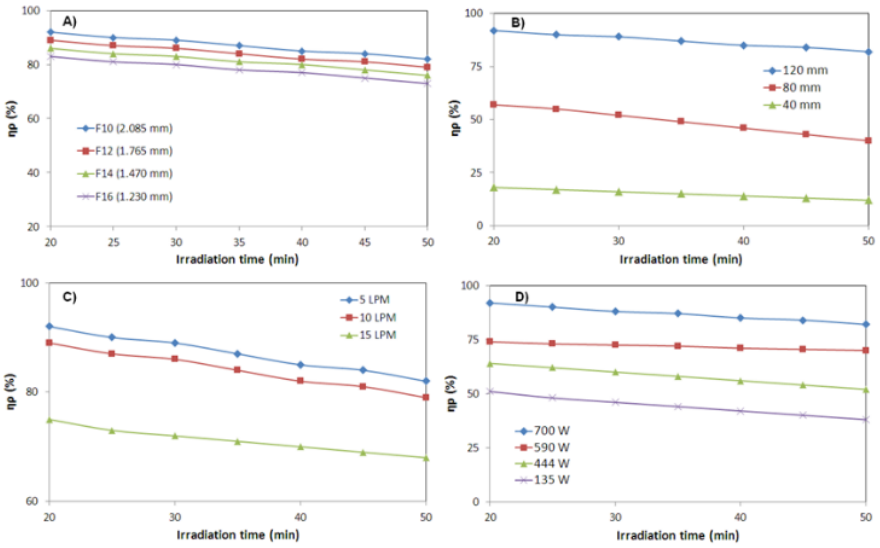

Figure 2. Power absorption efficiency for different: (a) SiC particle size, (b) SiC bed height, (c) gas flow rate, and (d) microwave input power

3.1.2.Effect of bed height

The effect of SiC bed height on the microwave oven power absorption efficiency was further characterized while fixing other variables at 10 LPM N_2 flow rate, F16 SiC particle size and 700 W power input. The absorption efficiencies were calculated with three bed heights as shown in Figure 2b. As expected, the absorption efficiency improved significantly as the volume of absorber bed material increased. It was found that the average power absorption efficiencies for bed heights of 40, 80 and 120 mm were 15%, 43% and 87%, respectively. Thus, it can be concluded that for lower bed height/volume, only a small portion of the emitted microwave power to the absorber material can be absorbed and converted into heat. On the other hand, increasing the height of the bed materials is limited by the reactor geometry and also by the elevation in flow pressure drop. SiC bed height of 120 mm was used in all subsequent experiments. Further increase of bed height was not possible due to the limitation of reactor size used in this work.

3.1.3.Effect of gas flow rate

Another significant variable is the gas flow rate through the reactor since it governs the residence time. Bed particle size or bed porosity usually affects directly the flow rate when low-pressure blower is used, due to the flow restriction. However, with pressurized N_2 used as the carrier gas, the pressure drop effect was eliminated. The effect of various N_2 flow rates in the range of 5 - 15 LPM were investigated while fixing other variables such as the maximum bed height of 120 mm, F16 SiC particle size and 700 W power input as shown in Figure 2c. It can be noticed that lower gas flow rate resulted in higher power absorption efficiency. This phenomenon can be explained by the heat balance within the reactor in which the microwave power dissipation into heat from the absorber material surface was still able to overcome the heat losses especially by convection. On the other hand, for high flow rates the flow cooling effect was significant causing a drop in temperature and absorption efficiency. The results show that the average power absorption efficiencies for gas flow rates of 5, 10 and 15 LPM were 92%, 87% and 66%, respectively. In

general, the required residence time for tar cracking will be the main factor that determines the suitable gas flow rate. However, these results give an insight on the flow rate effect on absorption efficiency where gas flow rates below 15 LPM is recommended to obtain better heating.

3.1.4.Effect of microwave power

The input power of the microwave is the primary variable that dictates the absorption power hence the absorption efficiency. Other variables were fixed at optimum values of 120 mm bed height, 10 LPM N_2 flow rate, and particle size of F16. Figure 2d shows the power absorption efficiency for different microwave input powers. The average absorption efficiencies for 135, 444, 590 and 700 W input powers were respectively around 41%, 54%, 67% and 87%. The rapid heating effect and fast temperature elevation at higher input powers resulted in a significant enhancement of the absorption efficiency compared to the low power operation.

It can be concluded that input power and bed height have more influence on power absorption efficiency followed by the gas flow rate then the bed particles sizes. Also a slight reduction in the absorption efficiency with time was noticed as a common trend for all the variables due to the slight changes in the absorber material properties with temperature elevation.

3.2. Effect of Catalyst and Water Addition on Tar Removal

Sufficient removal of tar contamination in biomass syngas using only heat supply from the microwave oven will require a significant temperature elevation up to 1200 ^{0}C. This might be not feasible both technically and economically in many large scale gas cleaning applications. Adding water has shown a considerable enhancement in tar removal efficiency, but high temperature was still a requirement [36]. Adding catalysts has been proven to achieve good tar cracking at much lower temperatures and hence, lower power input requirement. In this study, dolomite, Y-zeolite, nickel, ruthenium, and rhodium catalytic materials were all tested separately with S/C ratios in the range of 0.1- 0.5 and temperature range of 500-700 ^{0}C.

Figure 3 shows the removal efficiency for toluene and naphthalene with the various catalysts. The optimization temperature was limited to a relatively low cracking temperature of 700 ^{0}C rather than the maximum tested temperature of 900 ^{0}C. The lower temperature is more attainable from the practical point of view since the catalytic materials can be placed right after the throat in downdraft gasifiers where gas temperature is still around 700 ^{0}C before it cools down at the gasifier exit. This eliminates the need for external heating for the tar cracking purpose. Steam addition triggers the water-gas shift reaction, even at lower reaction temperatures due to the low energy required for the activation, and the reaction increases H_2 and CH_4 concentrations in the gas. On the other hand, steam reforming reaction requires higher energy for the activation and the inclusion of this reaction in the overall reaction equilibrium is limited and depends on the local temperature of the reactants.

Increasing S/C ratio contributed positively to the tar removal for all the catalysts up to 0.33 ratio. However, further increase in steam flow showed the opposite effect on tar cracking. This could be attributed to the coke formation at higher steam flow rates as early studies in literature reported the increase of coke deposits on catalyst surface resulted from the steam reforming reaction at lower temperatures [44]. The type of catalyst also plays a major role in the resistance toward coke formation on the surface that can lead eventually to the catalyst deactivation.

Therefore, an adequate presence of steam to initiate tar cracking through the water-gas shift as the main reaction and partially through the steam reforming reaction was found to be at S/C ratio in the range of 0.32-0.33 for toluene and naphthalene. Further increase of steam flow increased the steam reformation activation in the global equilibrium. This resulted in the formation of coke deposits on the catalysts surfaces with noticeable degradation in the tar cracking performance. The most effective catalyst was ruthenium followed by nickel. Average toluene removal efficiencies for the optimum condition for the catalysts were: 97.27% for dolomite, 96.04% for Y-zeolite, 96.55% for rhodium, 98.76% for nickel, and 98.88% for ruthenium. As for naphthalene, the effect of the catalyst type was nearly identical to that of toluene with both having similar number of hydrogen atoms. However, with naphthalene being heavier than toluene, the maximum naphthalene removal efficiency was slightly lower of 96.9%.

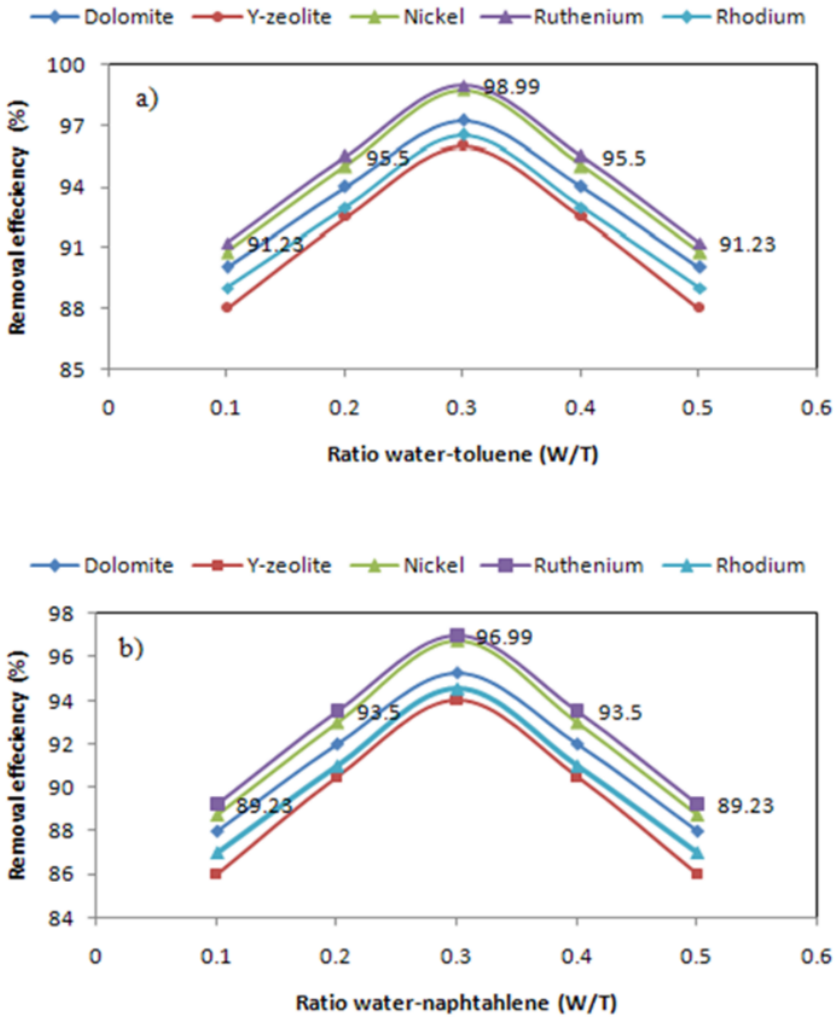

Figure 3. The effect of water addition on tar removal efficiency with various types of catalysts for toluene and naphthalene

Tar removal efficiencies were compared for the cases with S/C ratio range of 0.32-0.33 and without any water addition with all the catalysts at 700 ^{0}C as shown in Figure 4. It can be noticed that naphthalene which is class 4 tar was much harder to crack compared to the lighter toluene, a class 3 tar in all the cases. Also, up to 4.9% enhancement in removal efficiency for both naphthalene and toluene were achieved by adding the optimum amount of water to the reaction with ruthenium.

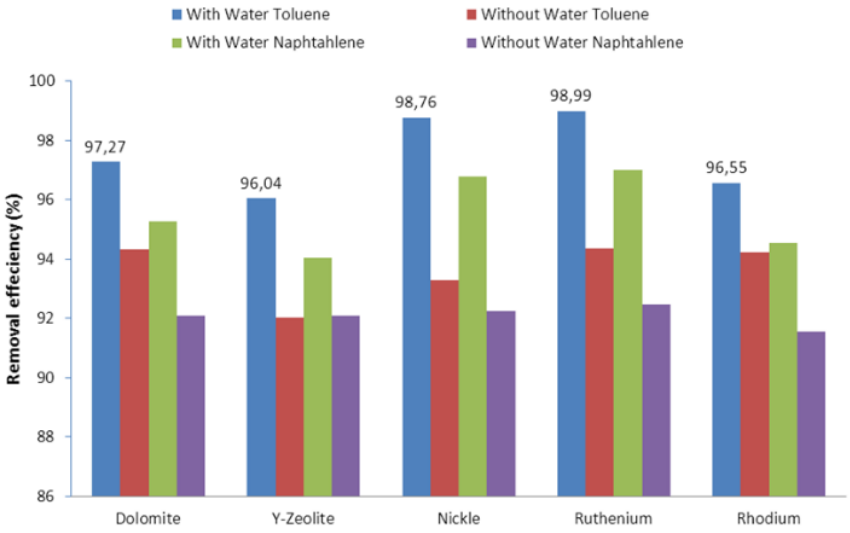

Figure 4. Removal efficiency of tar models with different type of catalysts at 700 ^{0}C and residence time of 0.24s

Most of the tar model was converted into a gas product inside the reactor, while the remaining condensable tar was collected in the sampling train and analysed using GC-MS. Table 2 shows the species mass concentrations of the remaining condensable tar reduced from toluene after the catalytic thermal treatment with ruthenium and water in the temperature range of 500-700 ^{0}C. It was found that most of toluene mass was converted into different tar species during thermal treatment except for the samples treated at 700 ^{0}C where 45% of toluene remained in the sample. This finding is slightly different to the detected tar species in the case of dolomite at 700 ^{0}C in which phenanthrene, styrene and chrysene were not identified in the case of ruthenium at 500 ^{0}C. In addition, most of the heavy PAHs were decomposed at reaction temperature of 500 ^{0}C, meaning that the ruthenium catalyst inhibited the formation of high-ring tar compounds. This activity was due to Y-zeolite catalyst contained sufficient acidic active sites on its surface thereby accelerated tar cracking reaction. Moreover, by increasing the catalytic reaction temperature up to 700 ^{0}C, it can be seen that the catalytic activities of ruthenium increased significantly. At this condition, benzene, toluene, o-xylene, indene, methylindene and naphthalene were the only major compounds identified.

Table 2. Tar sample compound and composition resulting from ruthenium catalytic treatment of model tar toluene

Compound name	Molecular weight	Boiling point (°C)	Tar sample composition after cracki Ruthenium catalyst reaction temper:			
			500	550	600	650
Benzene	78	80	11.45	9.57	14.35	10.69
Toluena	92	110.6	13.63	11.19	12.15	16.93
Ethylbenzene	106	145	0.85	0.87	-	-
p-Xylene	106	138.3	1.31	1.80	1.94	2.95
o-Xylene	106	144.5	2.87	3.62	4.65	6.59
Benzene, (1-methylethyl)-	120	172.8	0.19	0.16	-	-
Indene	116	182	6.54	6.50	7.27	2.82
Methylindene	130	199	7.87	11.04	4.88	4.69
Naphthalene	128	217.9	4.27	6.39	6.54	7.90
2-Methylnaphthalene	142	241.1	3.01	5.84	4.88	5.66
1-Methylnaphthalene	142	244.7	2.10	5.88	4.33	2.61
4-Butyl-1,1'-biphenyl	210	318	2.54	-	-	-
Anthracene	178	339.9	4.50	10.33	6.96	-
Methylenephenanthrene	190	353	4.03	5.71	7.17	-
Fluoranthene	202	384	3.23	5.71	4.44	-
Pyrene	202	404	6.29	8.22	11.75	26.00
11H-Benzo|b|fluorene	216	405	7.56	7.15	8.70	13.17
Pyrene, 1-methyl-	216	405	6.25	-	-	-
Acepyrene	226	448	11.48	-	-	-
Total			100	100	100	100

3.3. Gas Product Characteristics

The last set of experiments included the optimization of the gas product from toluene and naphthalene tar model compounds. Different types of catalysts were tested in the temperature range of 500 - 700 ^{0}C, gas residence time in the range of 0.12 - 0.24 seconds and optimum S/C ratio range of 0.32-0.33. It was found that dolomite and rhodium showed low toluene removal efficiency compared to Y-zeolite, nickel and ruthenium at the conditions investigated. Same goes for the removal of naphthalene that showed similar behaviour which is also in a good agreement with the findings of other researchers [27].

Differences in the catalyst activity were mainly due to the differences in their physical and chemical properties shown earlier in Table 1. The literature suggests that the average pore diameter of dolomite is generally above 600 μm while Y-zeolite has a pore size of about 7.4 μm [16]. On the other hand, toluene and naphthalene molecules are in the range of 0.49-0.73 μm. Thus, the porous structure of Y-zeolite, ruthenium and rhodium catalysts with larger pore size allows toluene and naphthalene to diffuse into the pores causing higher catalytic activity. Moreover, the high activity of these catalysts can also be contributed by its higher contact surface area, additional to the acidic nature of the catalysts that can also promote the removal of toluene and naphthalene. On the other hand, dolomite and nickel suffered from the non- porous structure that limited the contact surface area.

Toluene removal efficiency with different catalysts and gas products yield mainly H_2, CH_4 and higher HCs as shown in Figures 5 a-e. The removal of toluene was carried out in the temperature range of 700 - 900 ^{0}C for dolomite and nickel and 500-700 ^{0}C for Y zeolite, ruthenium, and rhodium. The lower removal efficiency with dolomite and nickel need

temperature elevation up to 900 ^{0}C to get higher efficiency comparable to the other catalysts. Soot was observed on dolomite and nickel surfaces with a small portion of the catalysts turned black, especially at the bottom. This can be explained by the higher pore size with less contact surface area for the reaction resulting in concentrated reaction hot spots. Also, Y-zeolite requires lower temperatures (maximum 700 ^{0}C) while the other catalyst materials have low Si/Al ratios such as A-, X and high ratio of Si/Al such as ZSM-5 that requires higher temperatures up to 1300 ^{0}C. Further increase in temperature showed no significant improvement in toluene removal for all the cases. The black grains and soot products decreased significantly with the increase in temperature during the toluene and naphthalene removal with Y zeolite, ruthenium, and rhodium. This is mainly due to the larger contact surface area for reaction and the acidic nature the catalysts.

Removal of toluene showed a significant improvement at higher temperatures for all catalysts. As for the gas production, a steady elevation in H_2 was noticed mainly due to the water addition through the steam reforming and water gas shift reactions. On the other hand, significant elevation in CH_4 production was noticed at higher temperatures mainly due to the cracking of higher HCs that converted eventually to H_2 and CH_4. This could also be partially attributed to the slower methane dry reforming reaction compared steam reactions [45] that reduced CH_4 conversion into H_2 and CO. The effect of catalytic materials used here on tar cracking can be put in the order from highest to lowest as following: ruthenium, nickel, dolomite, rhodium, and Y zeolite. In conclusion, the main factors contributed to the high efficiency tar removal were the intensive radio frequency heating, long residence time, high temperature and catalytic materials.

The use of catalytic materials inside the gasifier chamber for tar cracking has the advantage of the elevated temperature and the availability of steam released from the raw materials during the initial drying phase. However, this method suffers from the frequent deactivation of the catalysts caused by the coke and alkaline materials deposits on the catalyst surface. Tar contamination in gas product from updraft gasifiers occurs when gas passes through the relatively cooler pyrolysis and drying zones. Thus, tar contains mainly heavy oxygenated-based compounds and heterocyclic compounds presenting classes 1 and 2 which can be efficiently removed using second stage thermal cracking reactor. On the other hand, the oxygenated light tar compounds are cracked when the gas passes through the hot throat in downdraft gasifiers, leaving only tars of classes 3 and 4 in the gas. A combination of a catalyst with oxygen carrier materials can be placed at the gasifier throat exit with external steam stream at an adequate S/C ratio can be a promising solution since the gas temperature is still above 700°C. This will not only reduce the tar contamination, but also enhance the quality of the gas product by elevating the H_2 and CH_4 concentrations in the gas.

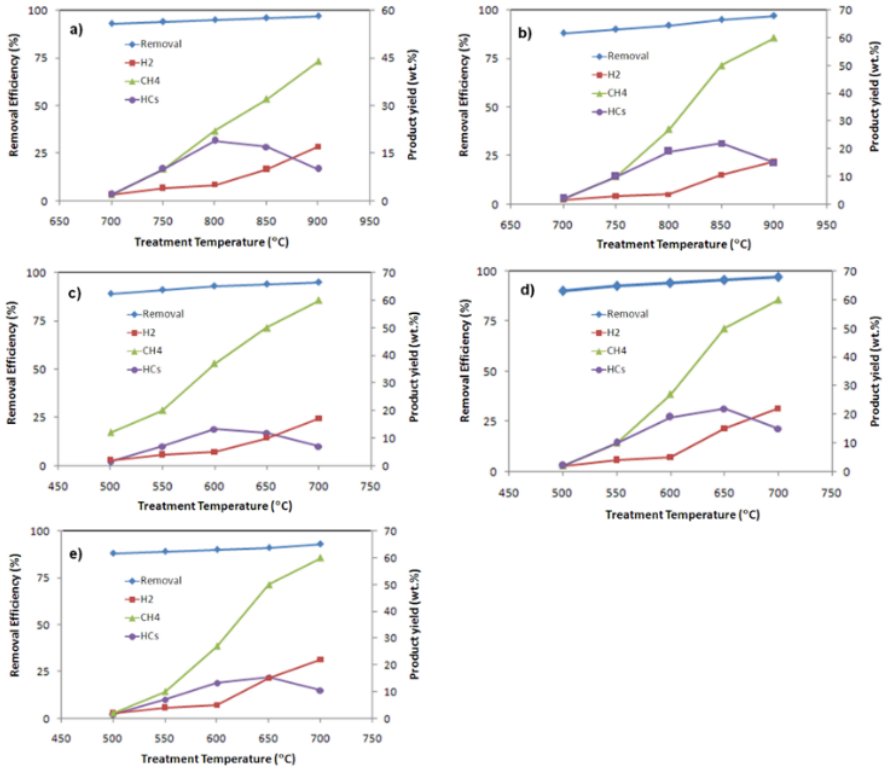

Figure 5. The final product during catalyst removal tar model of toluene with catalysts: (a) dolomite and (b) nickel (c) Y-zeolite, (d) ruthenium and (e) rhodium

4. Conclusions

Microwave assisted hydro-catalytic biomass tar cracking was experimentally investigated. The microwave reactor optimum operation condition were found to be 700 W input power, 120 mm bed height and 5LPM carrier gas flow rate with maximum power absorption efficiency of 87%. Optimum S/C ratio was in the range of 0.32-0.33 for naphthalene and toluene tar models with maximum tar removal efficiency of 98.88% with ruthenium catalyst at 700 °C. Gas product from tar cracking was characterized in the temperature range of 500–700 °C. CH_4 yield was above 50% with most of the catalysts and dropped with dolomite, while H_2 was about 20% for most of the catalysts and dropped with nickel.

Acknowledgments: The author would like to thank Universiti Sains Malaysia and FRGS 203/PMEKANIK/6071320 for the financial support of this work.

References

1. Al-attab KA, Zainal ZA (2017) Syngas production and combustion characteristics in a biomass fixed bed gasifier with cyclone combustor. Appl. Therm. Eng. 113, 714–721.
2. Grieco EM, Gervasio C, Baldi G (2013) Lanthanum–Chromium–Nickel Perovskites for the Catalytic Cracking of Tar Model Compounds. Fuel 103, 393–397.
3. Al-attab KA, Zainal ZA (2014) Performance of a biomass fueled two-stage micro gas turbine (MGT) system with hot air production heat recovery unit. Appl. Therm. Eng. 70, 61- 70.

4. Mastellone ML, Zaccariello L (2013) Metals Flow Analysis Applied to the Hydrogen Production by Catalytic Gasification of Plastics. Int. J. Hydrogen Energy 38, 3621–3629.
5. Ud Din Z, Zainal ZA (2016) Biomass integrated gasification–SOFC systems: Technology overview, Renewable Sustainable Energy Rev. 53, 1356–1376.
6. Anis S, Zainal, ZA. (2011) Tar reduction in biomass producer gas via mechanical, catalytic and thermal methods: A review. Renew. Sustain. Energy Rev. 15, 2355-2377.
7. Machin EB, Pedroso DT, Proenza N, Silveira JL, Conti L, Braga LB, Machin A B (2015) Tar reduction in downdraft biomass gasifier using a primary method. Renew. Energy 78, 478-483.
8. Zhang Y, Kajitani S, Ashizawa M, Oki Y (2010) Tar destruction and coke formation during rapid pyrolysis and gasification of biomass in a drop-tube furnace. Fuel 89, 302-309.
9. Zhang Z, Liu L, Shen B, Wu C (2018) Preparation, modification and development of Ni-based catalysts for catalytic reforming of tar produced from biomass gasification. Renewable and Sustainable Energy Reviews 94, 1086–1109.
10. Xu J, Holthaus P, Yang N, Jiang S, Heupel A, Schönherr H, Yang B, Krumm W, Jiang X (2019) Catalytic tar removal using TiO2/NiWO4-Ni5TiO7 films. Applied Catalysis B: Environmental 249, 155-162.
11. Sutton D, Kelleher B, Ross JR (2001) Review of Literature on Catalysts for Biomass Gasification. Fuel Process. Technol. 73, 155–173.
12. Asadullah M, Miyazawa T, Ito SI, Kunimori K, Yamada M, Tomishige K. (2003) Catalyst Development for the Gasification of Biomass In The Dual-Bed Gasifier. Appl. Catal., A. 255, 169–180.
13. Rapagná S, Provendier H, Petit C, Kiennemann A, Foscolo PU (2002) Development of Catalysts Suitable for Hydrogen or Syn-Gas Production from Biomass Gasification. Biomass Bioenergy 22, 377-388.
14. Taralas G, Kontominas MG (2006) Pyrolysis of Solid Residues Commencing from the Olive Oil Food Industry for Potential Hydrogen Production. J. Anal. Appl. Pyrolysis 76, 109–116.
15. Pérez-Martínez D, Giraldo SA, Centeno A (2006) Effects of The H2S Partial Pressure on The Performance of Bimetallic Noble-Metal Molybdenum Catalysts in Simultaneous Hydrogenation And Hydrodesulfurization Reactions. Appl. Catal., A. 315, 35–43.
16. [Aznar MP, Caballero MA, Sancho JA, Francés E (2006) Plastic Waste Elimination By Co-Gasification With Coal And Biomass in Fluidized Bed With Air in Pilot Plant. Fuel Process. Technol. 87, 409–420.
17. Gusta E, Dalai AK, Uddin MA, Sasaoka E (2009) Catalytic Decomposition of Biomass Tars with Dolomites. Energy Fuel 23, 2264–2272.
18. Devi L, Ptasinski KJ, Janssen FJ, Van Paasen SV, Bergman PC, Kiel JH (2005) Catalytic Decomposition of Biomass Tars: Use of Dolomite and Untreated Olivine. Renew. Energy 30, 565–587.
19. Chiang KY, Lu CH, Lin MH, Chien KL (2013) Reducing Tar Yield in Gasification of Paper-Reject Sludge by Using A Hot-Gas Cleaning System. Energy 50, 47–53.
20. Mun TY, Kim JS (2013) Air gasification of dried sewage sludge in a two-stage gasifier. Part 2: Calcined dolomite as a bed material and effect of moisture content of dried sewage sludge for the hydrogen production and tar removal. Int. J. Hydrog. Energy 38, 5235–5242.
21. Mun TY, Kim JW, Kim JS (2013) Air gasification of dried sewage sludge in a two-stage gasifier: Part 1. The effects and reusability of additives on the removal of tar and hydrogen production. Int. J. Hydrog. Energy 38, 5226–5234.
22. Ud Din Z, Zainal ZA (2017) The fate of SOFC anodes under biomass producer gas contaminants. Renew. Sustain. Energy Rev. 72, 1050–1066.
23. Chang JS (2003) Next Generation Integrated Electrostatic Gas Cleaning Systems. J. Electrostatic. 57 273–291.
24. Ribeiro AM, Santos JC, Rodrigues AE (2010) PSA Design for Stoichiometric Adjustment of Bio-Syngas for Methanol Production and Co-Capture of Carbon Dioxide. Chem. Eng. J. 163 355–363.

25. Bu Q, Lei H, Zacher AH, Wang L, Ren S, Liang J, Wei Y, Liu Y, Tang J, Zhang Q, Ruan R (2012) A Review of Catalytic Hydrodeoxygenation of Lignin-Derived Phenols from Biomass Pyrolysis. Bioresour. Technol. 124, 470–477.
26. Wang, L., Li, D., Koike, M., Koso, S., Nakagawa, Y., Xu, Y., Tomishige, K.: Catalytic Performance And Characterization of Ni-Fe Catalysts for The Steam Reforming of Tar From Biomass Pyrolysis To Synthesis Gas. Appl. Catal., A. 392, 248–255 (2011).
27. Farag S, Kouisni L, Chaouki J (2014) Lumped Approach in Kinetic Modeling of Microwave Pyrolysis of Kraft Lignin. Energy Fuels 28, 1406–1417.
28. Anis, S., Zainal, Z. A., Bakar, M. Z. A.: Thermocatalytic Treatment of Biomass Tar Model Compounds via Radio Frequency. Bioresour. Technol. 136, 117–125 (2013).
29. Anis S, Zainal ZA (2013) Upgrading producer gas quality from rubber wood gasification in a radio frequency tar thermocatalytic treatment reactor, Bioresour. Technol. 150, 328–337.
30. Li L, Song Z, Zhao X, Ma C, Kong X, Wang F (2016) Microwave-induced cracking and CO2 reforming of toluene on biomass derived char, Chem. Eng. J. 284, 1308–1316.
31. Feng D, Zhao Y, Zhang Y, Sun S, Meng S, Guo Y, Huang (2016) Effects of K and Ca on reforming of model tar compounds with pyrolysis biochars under H2O or CO2, Chem. Eng. J. 306, 422–432.
32. Bhattacharya M, Basak T (2016) A review on the susceptor assisted microwave processing of materials. Energy 97, 306 338.
33. Radwan AM, Kyotani T, Tomita A (2000) Characterization of Coke Deposited from Cracking of Benzene over Usy Zeolite Catalyst. Appl. Catal., A. 192, 43–50.
34. Buchireddy PR, Bricka RM, Rodriguez J, Holmes W (2010) Biomass Gasification: Catalytic Removal of Tars Over Zeolites and Nickel Supported Zeolites. Energy Fuels 24, 2707–2715.
35. Anis S, Zainal ZA (2014) Study on kinetic model of microwave thermocatalytic treatment of biomass tar model compound, Bioresour. Technol. 151, 183–190.
36. Lv P, Chang J, Xiong Z, Huang H, Wu C, Chen Y, Zhu J (2003) Biomass Air−Steam Gasification in a Fluidized Bed to Produce Hydrogen-Rich Gas. Energy Fuels 17, 677–682.
37. Hu G, Xu S, Li S, Xiao C, Liu S (2006) Steam gasification of apricot stones with olivine and dolomite as downstream catalysts. Fuel Process. Technol. 87, 375-382.
38. Warsita A, Al-attab KA, Zainal ZA (2017) Effect of water addition in a microwave assisted thermal cracking of biomass tar models, Appl. Therm. Eng. 113, 722–730.
39. Cherbanski R, Molga E (2009) Intensification of desorption processes by use of microwaves—An overview of possible applications and industrial perspectives. Chem. Eng. Process. 48, 48–58.
40. Li C, Hirabayashi, D, Suzuki K (2009) A crucial role of O2 - and O2 2- on mayenite structure for biomass tar steam reforming over Ni/Ca12Al14O33. Appl. Catal. B: Environ. 88, 351-360.
41. Virginie M, Adánez J, Courson C, De Diego LF, García-Labiano F, Niznansky D, Kiennemann A, Gayán P, Abad A (2012) Effect of Fe–Olivine on The Tar Content During Biomass Gasification in A Dual Fluidized Bed. Appl. Catal., B. 121–122, 214–222.
42. Virginie M, Courson C, Kiennemann A (2010) Toluene Steam Reforming as Tar Model Molecule Produced During Biomass Gasification with An Iron/Olivine Catalyst. C. R. Chim. 13, 1319–1325.
43. Skoulou V, Kantarelis E, Arvelakis S, Yang W, Zabaniotou A (2009) Effect of Biomass Leaching on H2 Production, Ash And Tar Behavior During High Temperature Steam Gasification (Htsg) Process. Int. J. Hydrog. Energy 34, 5666–5673.
44. Trimm DL (1997) Coke formation and minimisation during steam reforming reactions. Catalysis Today, 37, 233-238.
45. Kajitani, S., Suzuki, N., Ashizawa, M. & Hara, S. 2006. CO_2 gasification rate analysis of coal char in entrained flow coal gasifier. Fuel, 85, 163-169.

Hydro-Catalytic Cracking of Biomass Tar Contamination in Syngas

ORIGINALITY REPORT

24%	17%	18%	4%
SIMILARITY INDEX	INTERNET SOURCES	PUBLICATIONS	STUDENT PAPERS

MATCH ALL SOURCES (ONLY SELECTED SOURCE PRINTED)

4%

★ c.coek.info

Internet Source

Exclude quotes	Off	Exclude matches	Off
Exclude bibliography	On		